

# Shape and Positional Anisotropy based Area Efficient Magnetic Quantum-dot Cellular Automata Design Methodology for Full Adder Implementation

Santhosh Sivasubramani, Venkat Mattela, Chandrajit Pal, M. Saif Islam, *Senior Member, IEEE*,  
Amit Acharyya, *Member, IEEE*

**Abstract**—Magnetic Quantum-dot Cellular Automata (MQCA) based computation started emerging as the Moore’s law approaching towards its end. Number of nanomagnets and the area occupancy are major constraints in materializing this MQCA based digital arithmetic circuit design. In this letter, we propose a design methodology and demonstrate the hybrid approach of using slant edged input and 45 degree aligned nanomagnets for optimized binary full adder design. Asymmetric shape anisotropy nanomagnets pave the way for standalone inputs, whereas positional anisotropy reduces the signal loss in transmission of data and enables lossless information propagation. This complementary property of both shape and positional anisotropy lead to exploiting the energy minimization nature of nanomagnets, reducing the design footprint. Further, to enable the multipurpose scaling, horizontal and vertical layouts of the nanomagnetic computing design of full adder has been proposed. Our proposed nanomagnetic adder architecture leads to 28% reduction in the total number of nanomagnets compared to the state of the art design, leading to an area efficient architectural design.

**Index Terms**—Adder, Area efficient, Magnetic Quantum-dot Cellular Automata (MQCA), Nanomagnetic computing, Optimization, Positional anisotropy (P), Shape anisotropy (S)

## I. INTRODUCTION

CELLULAR Automata (CA) controls information flow through the interaction of cell between the nearest-neighbors. The information is stored in the cell’s state, in contrast to the approach of traditional computing paradigm. Physical realization of these cells is achieved by field coupled ferromagnetic single domain dots using magnetic dipolar

Manuscript received May 24, 2018; revised August 10, 2018 and accepted October 2, 2018

This work was supported partly by the Redpine Signals, Inc. USA (Grant No: Redpine/EE/F091/2017-18/S22) and NPDF, Govt. of India. Amit Acharyya would like to acknowledge his Visvesvaraya Young Faculty Fellowship Award from the Ministry of Electronics and Information Technology (MEITY), Government of India (GOI). SMDP, MEITY, GOI is acknowledged for supporting computational tools.

S. Sivasubramani, V. Mattela, C. Pal and A. Acharyya are with the Advanced Embedded Systems and IC Design Laboratory, Department of Electrical Engineering, IIT Hyderabad, Hyderabad 502285, India (e-mail:ee15m16p100001,ee17resch11018,ee17pdf04,amit\_acharyya@iith.ac.in).

M. S. Islam is with the Integrated Nanodevices and Nanosystem Research Group, Department of Electrical and Computer Engineering, University of California, Davis, CA 95616 USA (e-mail: sislam@ucdavis.edu).

Copyright (c) 2018 IEEE. Personal use of this material is permitted. However, permission to use this material for any other purposes must be obtained from the IEEE by sending a request to [pubs-permissions@ieee.org](mailto:pubs-permissions@ieee.org). Color versions of one or more of the figures in this paper are available online at <http://ieeexplore.ieee.org>.

Digital Object Identifier:

interactions [1]. Computing with magnetic dots (nanomagnets) would be so efficient, that they would consume the least amount of energy allowed by the second law of thermodynamics demonstrating the Landauer limit. They also retain their magnetic states (non-volatile property) when powered off. This energy efficient NanoMagnetic Computing paradigm has started emerging after the room temperature realization of Magnetic Quantum-dot Cellular Automata (MQCA) [2]–[4].

Logic functionalities have been demonstrated by the implementation of universal logic gates using MQCA based majority logic with ferromagnetic dots [5]. Thereafter, researchers started realizing interconnects using the dipole-coupled single domain nanomagnets [6]–[8] leading to ultra-low power, non-volatile irradiated device [9], [10]. The on-chip implementation of MQCA was shown by Alam et al., by replacing the driver magnets with the copper wire [11] to reduce the area overhead. Researchers realized the digital arithmetic circuits using these MQCA based universal logic gates [12]. Yang et al., [13] designed MQCA adder using NWS (North, West and South)-direction-input gate (M1), two NWE (North, West and East)-direction-input gates (M2 and M3), and two inverters. Gradually shape engineering [14]–[18] of the nano-structured magnets started evolving for optimizing the MQCA based circuit design. Varga et al., [19] proposed the concept of slanted edge magnets as part of the shape engineering and implemented adder using this to optimally utilize the number of nanomagnets. Very recently, positional anisotropy [20]–[22] of the nanomagnets began to originate for minimizing the signal attenuation and clocking field misalignment in the MQCA circuits. Zheng Li et al., [23] for the first time proposed MQCA based adder implementation using inclined clocking field with 45 degree alignment minimizing the operational error rate.

Motivated by the aforementioned facts, we propose a design methodology for implementing the binary full adder with a hybrid approach of utilizing shape and positional anisotropy of the nanomagnets leading to the optimized number of nanomagnets resulting in the reduction of area overhead. This letter is organized as follows: section II contains the proposed methodology, section III briefs the results and discussion and section IV concludes this letter.

## II. PROPOSED METHODOLOGY

State of the art MQCA based adder circuits are built utilizing the shape ( $S$ ) [19] and positional ( $P$ ) [23] anisotropy

of the single domain nanomagnets independently. Till date, the combined dependence of the shape and position of nanomagnets in the circuit design has not been investigated. We envisage here that the self-dependency of  $S$  and  $P$  will have its impact on design optimization. Motivated by the aforementioned facts, here we propose a design methodology of using  $SP$  hybrid field coupled nanomagnets for the binary full adder implementation.

The full adder [24] is designed using the logic functionalities expressed as in equation (1) and equation (2) where the inputs -  $A$ ,  $B$  are the operands and  $C_i$  is the carry in and the outputs -  $C_o$  is the carry out and  $S$  is the sum of the full adder.

$$C_o = AB + BC_i + AC_i \quad (1)$$

$$S = ABC_i + A'B'C_i + A'BC'_i + AB'C'_i \quad (2)$$

The architectural design of the full adder based on the majority logic of the inputs  $A$ ,  $B$ ,  $C_i$  is shown in Fig.1(a). To enable two input logic operations,  $C_i$  is used as a handle to set constant values of 0 and 1 performing two different logic operations [(N)AND/(N)OR]. We propose the hybrid approach of slant edged input nanomagnets (as part of the shape anisotropy) and 45 degree aligned information propagation nanomagnets of varying length (as part of the positional anisotropy) to optimize the required number of nanomagnets in the design. This combined effect of slant edged input magnet and 45 degree inclined magnet helps us to achieve the standalone inputs (without the driver magnet) and signal propagation with less attenuation in comparison to the state of art. We

ology namely Horizontal layout [23] (row based design as shown in Fig.1(b)) and Vertical layout [19] (column based design as shown in Fig.1(c-j)) enabling the multi-dimensional scalability. M1 (Blue), M2 (Green) and M3 (Orange) are the three majority gate functions required for the full adder implementation as represented in Fig.1(a). In the horizontal layout design as shown in Fig.1(b), majority gate (M3) is sandwiched between the majority gates (M1) and (M2). The design requires two 45 degree inclined magnets propagating the signal in North-East (NE) and South-East direction (SE) for antiferromagnetic coupling, representing the NOT function. To design the column based layout, the inputs of majority gates (M1, M2) are constituted by the slanted edge standalone input magnets. The majority gate (M3) has one standalone input magnet and two oval input magnets which are driven by the output of M1 and M2 as shown in Fig.1(c-j). This design also requires North-East and South-East positioned 45 degree inclined magnets for the signal propagation from M1 and M2 to act upon M3. Out of these two, the magnet ( $IC_1$ ) is coupled antiferromagnetically ( $C_o \Rightarrow C'_o$ ) and the magnet ( $IC_2$ ) by ferromagnetic means ( $ABC'_i \Rightarrow ABC'_i$ ) to satisfy the logic functionalities as given in equations (1) and (2). Fig.1(c-j) illustrates all the possible combinations of the proposed adder design. The logic functionalities of equations (1) and (2) has been depicted in the Table I.

TABLE I  
TRUTH TABLE FOR THE BINARY FULL ADDER

Input			Output	
A	B	Carry In ( $C_i$ )	Carry out ( $C_o$ )	Sum (S)
0	0	0	0	0
0	1		0	1
1	0		0	1
1	1		1	0
0	0	1	0	1
0	1		1	0
1	0		1	0
1	1		1	1

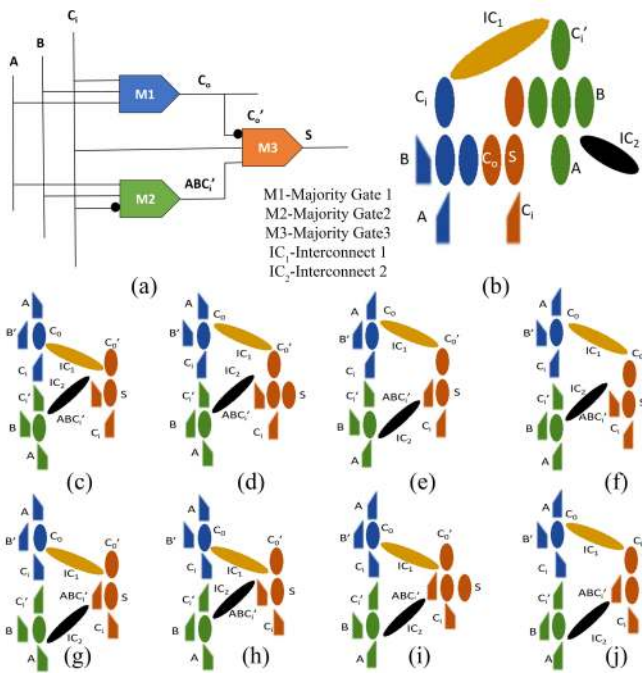


Fig. 1. a) Binary full adder circuit design b) Proposed horizontal layout of the nanomagnetic computing adder architecture (c) - (j) Proposed vertical layout of the nanomagnetic computing adder architecture to test the all 8 possible combinations (Blue accent Color 5 - Majority gate1; Green accent color 6 - Majority gate2; Orange accent color 2 - Majority gate3; Gold accent color 4 - Interconnect1 and Black - Interconnect2)

introduce here, two different layouts of MQCA design method-

We used Object Oriented MicroMagnetic Framework (OOMMF) [25] developed at ITL by NIST for the computational architecture study on full adder. Few commercialized micromagnetic simulation tools do exist, however with the plethora of available literatures [4]–[14], [16]–[19], [22], [26]–[28], we opted for the open source tool OOMMF. OOMMF uses Finite Difference method to solve the Landau-Lifshitz Gilbert (LLG) equations. 4th order Runge Kutta evolver is used as a time evolver to solve this ordinary differential equation. The value of maximum torque is set to  $10^{-5}$  A/m in lieu of time. Stoner Wohlfarth model has been selected to solve the rotation of magnetization in the single-domain behavior of nanomagnets. Magnetic anisotropic energy originates with the interaction referred as spin orbit coupling. Magnetic dot used throughout this study is of Permalloy (Py) comprising 78.5% nickel, 21.5% iron [29]–[32] which is a pronounced soft ferromagnetic material with low coercive field by nature. As its exchange energy is larger than the magnetocrystalline anisotropy and low magnetic anisotropy energy (MAE), the exchange interaction dominates the magnetic anisotropy. Permalloy possess zero

(0) uniaxial anisotropy constant, in line with this magnetic anisotropy greatly depends on the shape of the dot and it tends to align to its easy axis. The exchange Hamiltonian on this single domain nanomagnets requires high axial symmetry to maintain the magnetic anisotropy. We have used an exchange stiffness constant of  $13 \times 10^{-12}$  J/m, damping coefficient of 0.25 and saturation magnetization of  $800 \times 10^3$  A/m [33]. All the architectural designs has been modeled using CleWin [34] a hierarchical layout editor developed by WieWeb software. We have used 10 nm x 30 nm area; 10 nm thickness and 10 nm — 15 nm wall separation for oval magnets,  $15 \times 30 \times 10$  nm<sup>3</sup> dimensions for slant edged magnets and 50 nm, 70 nm varying length signal propagation nanomagnets inclined at 45 degree. Our proposed design methodology retains the potential to be fabricated experimentally as confirmed by [35], thus motivating this simulation study reported here on the sub 50nm design. The results obtained based on this OOMMF micromagnetic simulations are discussed in the next section.

### III. RESULTS AND DISCUSSION

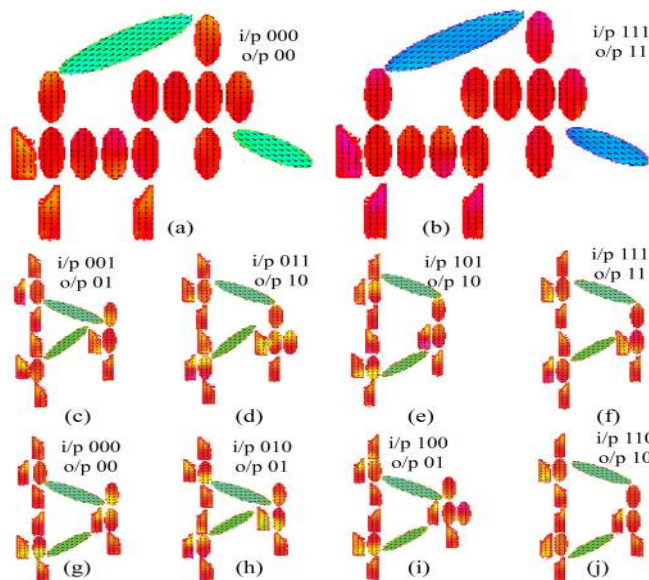


Fig. 2. a) OOMMF output for the horizontal layout of the nanomagnetic computing adder architecture with 0.5 Tesla of applied magnetic flux density (B) which demonstrates 000—00. b) OOMMF output for the horizontal layout of the nanomagnetic computing adder architecture output for -0.5 Tesla which demonstrates 111—11; Sign convention for all inputs and outputs Down as 1; Up as 0 and for input B Down as 0 and Up as 1. (c) - (j) Output for vertical layout of the nanomagnetic computing adder architecture design with B=0.5T; sign convention is Down as 0 and Up as 1.

The OOMMF simulation outputs of the horizontal layout of the nanomagnetic computing adder architecture is given in Fig. 2(a,b) for the applied flux density of 0.5 Tesla and - 0.5 Tesla respectively. The logic operations with input patterns 000 and 111 are given as a test structure. Fig.2(c-j) gives the output for the vertical layout of the nanomagnetic adder architecture. Slant edged magnets play a major role in acting as a standalone input magnet and the signal transmission takes

place effectively without error using 45 degree inclined magnets. All the possible combination of the logic functionalities has been shown to verify its successful operation. Fig.2(c-f) and Fig.2(g-j) shows the operation with  $C_i = 1$  and 0 respectively. To the best of our knowledge, this is the first of its kind of study which leads to 28% reduction in the number of nanomagnets for full adder implementation. The proposed design has been compared with the state of the art [12], [23] proposed adder designs with respect to the number of nanomagnets and majority gates utilized. The results are tabulated in Table II. Existing benchmark magnetic adder circuit design consists of 21 nanomagnets using 3 majority gate operations. The proposed horizontal and vertical layouts of the adder architecture lead to 16 (as in Fig.1(b)) and 14/15 (as in Fig.1(c-j)) nanomagnets respectively with 3 majority gate operations. Area occupancy of the proposed adder design is compared with the state of the art designs as tabulated in Table II. Adder designed by Varga et al., [19] utilizing the shape anisotropy of the nanomagnets occupies  $0.77015 \mu\text{m}^2$  area which is lesser than the design proposed by Zheng Li et al., [23] utilizing the positional anisotropy of the nanomagnets leading to  $1.96 \mu\text{m}^2$  of area occupancy. The proposed horizontal and vertical architectural designs are found to be occupying  $0.032175$  and  $0.031875 \mu\text{m}^2$  area respectively. Both the proposed layouts (horizontal and vertical) are equally comparable in terms of area occupancy. However the different layouts play a major role in System on Chip (SoC) applications where the scalable layouts are applicable for optimal placement (area utilization). The design proposed in [12] focus towards the footprint reduction however it faces issues while propagating data from majority gate 1 and 2 to majority gate 3 via interconnect magnets and the design in [23] focus on the clocking field misalignment however its area footprint could have been reduced further. The proposed hybrid approach of using shape and positional anisotropy of the nanomagnets put-forth a solution to bridge this gap between footprint reduction and low signal attenuation. The proposed optimization in the design enables the multi-dimensional scalability for applications in core areas of space exploration, communication devices, etc.

The usage of slant edged magnets [37] and the 45 degree alignment [21] are proved to maintain highly reliable structures independently. Intrinsic angular sensitivity in the hard axis, aids in increased tolerance against misalignment of the field and slanted edges helps in reliability when the dots are of modest size and requires smaller clocking field. Thus area reduction achieved by incorporating these designs possess inherent reliability. And moreover, our design requires only two clock cycles which also adds to the reliability. With the repeated simulations we found that the proposed design after space reduction is found to be error free and possess reliability. Thus our proposed area efficient adder design methodology is claimed to be reliable. Fig.3(a) presents the test loop design to verify the functionalities of shape and positional (SP) hybrid approach. Fig.3(b) exhibits the output state of the test loop design with applied magnetization of 0.5 Tesla in positive x-direction. Fig.3(c) shows the state of the output magnets with applied magnetization of 0.5 Tesla and reverse magnetization [38] of -0.15 Tesla. The outputs of O2 and O4 (as shown



TABLE II  
COMPARISON OF SELECTED NANOMAGNETIC ARCHITECTURES  
IMPLEMENTING FULL ADDERS WITH THE OPTIMIZED PROPOSED DESIGN

Design	Design Requirements	Design Strategy	Area Occupancy $\mu\text{m}^2$
[12]	21 nanomagnets <sub>a</sub>	Full adder with slant and regular oval-shaped magnets	0.77015 $\mu\text{m}^2$
[23]	21 nanomagnets <sub>a</sub>	Full adder with 45 degree and different aspect ratio input magnets	1.96 $\mu\text{m}^2$
Proposed <sub>1</sub> (Horizontal Layout)	16 nanomagnets <sub>a</sub>	Using 45 degree and slant edged magnets – horizontal layout design (Fig.1(b))	0.032175 $\mu\text{m}^2$
Proposed <sub>2</sub> (Vertical Layout)	14/15 nanomagnets <sub>a</sub>	Using 45 degree and slant edged magnets – vertical layout design (Fig.1(c-j))	0.031875 $\mu\text{m}^2$

<sub>a</sub> using 3 majority gates for sum and carry implementation together;  
1 Proposed Horizontal layout (Fig.1(b)) of the nanomagnetic computing adder architecture;  
2 Proposed Vertical layout (Fig.1(c-j)) of the nanomagnetic computing adder architecture

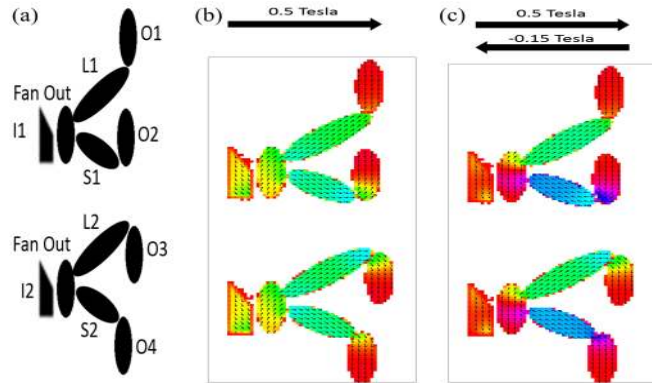


Fig. 3. a) Test loop design to demonstrate the advantages of the proposed hybrid approach of shape and positional anisotropy b) The output magnets (O1, O3) connected to longer (L1, L2) signal propagation magnets respectively and the output magnets (O2, O4) connected to shorter (S1, S2) signal propagation magnets respectively gives 1,0 and 1,0 on all outputs for 0.5 T c) With applied -0.15 T preceded by 0.5 T the received signal from S1 and S2 is flipped on the O2, O4 ( $1 \Rightarrow 0$  and  $0 \Rightarrow 1$ ) while O1, O3 connected to L1, L2 remains same ( $1 \Rightarrow 1$  and  $0 \Rightarrow 0$ ). This phenomenon occurs due to the nanomagnets inherent natural property of energy minimization [36] and different switching time of the magnetic states.

in Fig.3(c)) are flipped due to varying aspect ratios leading to different magnetic switching time. The role of 45 degree inclined signal propagation magnet ensures that the signal is not attenuated throughout the propagation. Fig.4 captures the flux density and normalized magnetization values for the horizontal (Fig.1(b)) and vertical layout (Fig.1(c-j)) of the nanomagnetic computing adder architectures. The exchange energy and demagnetization energy has been plotted against the applied flux density to study the energy minimization nature of the nanomagnets pertaining to low energy and ultra-low power switching. Fig.4(a) shows the energetics study along with the normalized magnetization against the applied magnetic flux. From this it is evident that the energy variations are negligible for the operation of both the horizontal (Fig.1(b)) and vertical layout design (Fig.1(c-j)). These two proposed design layouts, play a major role in design scalability as both have their different form factors. Fig.4b illustrates

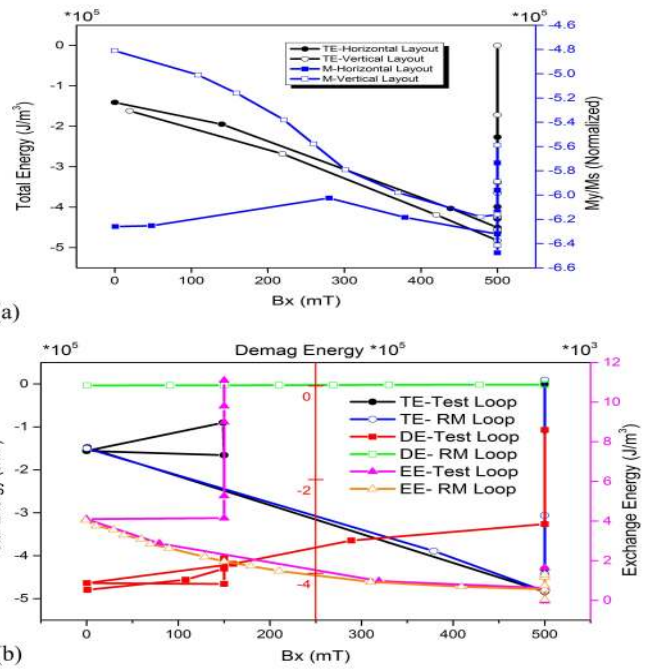


Fig. 4. a) BM curve for the horizontal layout of the nanomagnetic computing adder architecture and vertical layout of the nanomagnetic computing adder architecture with the coupled nanomagnetic energy difference for both the design b) Energetics study of the test loop design in applied magnetic flux and reversed magnetic flux. [TE, DE, EE = (Total, Demag, Exchange) Energy, RM - Reverse Magnetization, M=My/Ms]

the energy information of the test loop design. This helps us to confirm that the aspect ratio of the nanomagnets play a major role in signal propagation without attenuation. It has been observed that on applying -0.15 Tesla flips the state of the output magnet connected to the short signal propagation magnet, keeping the rest unchanged. Slant edged magnets plays a pivotal role in generating standalone inputs with the 45-degree inclination, further aiding in good signal propagation.

#### IV. CONCLUSION

28% reduction in the number of nanomagnets is achieved with the proposed hybrid design methodology leading to the area occupancy of  $0.032175\mu\text{m}^2$ . The proposed adder design has been tested successfully for all the 8 possible logic combinations using OOMMF based micromagnetic study. In spite of its proven earlier experimental realization, fabrication of the slant edged magnets (due to its sharp position at the edges) and positioning of 45 degree aligned magnets ( $\pm 5$  degree tolerability) will possess challenges. This arising experimental challenges could be handled with more precision and using high resolution state of the art lithographic tools. We envisage that the further optimization could be achieved on focusing towards the circuit level optimization and materialistic approach (2d materials [39]). We believe that the design methodology presented here possess the potential to be extended using Single Molecule Magnets (SMM) called as molecular nanomagnets and Molecular QCA (silicon phthalocyanine dimer) as part of molecular electronics. Quantum thermodynamic and resonant tunnelling will play a major role in

designing such systems [40]. *SP* hybrid area efficient MQCA design methodology introduced in this letter paves the path towards building higher dimensional nanomagnetic computing architectures like multipliers, filters etc and favorable to be deployed in low power portable design applications.

## REFERENCES

- [1] W. Porod and M. Niemier, "Better computing with magnets - The simple bar magnet, shrunk down to the nanoscale, could be a powerful logic device," *IEEE Spectrum*, vol. 52, pp. 44-60, 2015.
- [2] R. P. Cowburn and M. E. Welland, "Room temperature magnetic quantum cellular automata," *Science*, vol. 287, pp. 1466-1468, Feb 2000.
- [3] Cowburn, R. P., Probing antiferromagnetic coupling between nanomagnets. *Physical Review B* 2002, 65 (9), 092409.
- [4] G. Csaba, A. Imre, G. H. Bernstein, W. Porod, and V. Metlushko, "Nanocomputing by field-coupled nanomagnets," *IEEE Transactions On Nanotechnology*, vol. 1, pp. 209-213, 2002.
- [5] A. Imre, G. Csaba, L. Ji, A. Orlov, G. H. Bernstein, and W. Porod, "Majority logic gate for magnetic quantum-dot cellular automata," *Science*, vol. 311, pp. 205-208, Jan 2006.
- [6] Orlov, A.; Imre, A.; Csaba, G.; Ji, L.; Porod, W.; Bernstein, G. H., Magnetic Quantum-Dot Cellular Automata: Recent Developments and Prospects. *Journal of Nanoelectronics and Optoelectronics* 2008, 3 (1), 55-68.
- [7] E. Varga, A. Orlov, M. T. Niemier, X. S. Hu, G. H. Bernstein, and W. Porod, "Experimental Demonstration of Fanout for Nanomagnetic Logic," *IEEE Transactions on Nanotechnology*, vol. 9, pp. 668-670, 2010.
- [8] Pulecio, J. F.; Pendru, P. K.; Kumari, A.; Bhanja, S., Magnetic Cellular Automata Wire Architectures. *IEEE Transactions on Nanotechnology* 2011, 10 (6), 1243-1248.
- [9] Csaba, G.; Lugli, P.; Porod, W. Power dissipation in nanomagnetic logic devices, 4th IEEE Conference on Nanotechnology, 2004., 16-19 Aug. 2004; 2004; pp 346-348.
- [10] Niemier, M.; Alam, M.; Hu, X. S.; Bernstein, G.; Porod, W.; Putney, M.; DeAngelis, J. Clocking structures and power analysis for nanomagnet-based logic devices, Low Power Electronics and Design (ISLPED), 2007 ACM/IEEE International Symposium on, 27-29 Aug. 2007; 2007; pp 26-31.
- [11] M. T. Alam, M. J. Siddiq, G. H. Bernstein, M. Niemier, W. Porod and X. S. Hu, "On-Chip Clocking for Nanomagnet Logic Devices," in *IEEE Transactions on Nanotechnology*, vol. 9, no. 3, pp. 348-351, May 2010. doi: 10.1109/TNANO.2010.2041248
- [12] E. Varga, G. Csaba, G. H. Bernstein, and W. Porod, "Implementation of a nanomagnetic full adder circuit," in 2011 11th IEEE International Conference on Nanotechnology, 2011, pp. 1244-1247.
- [13] X. Yang, L. Cai, and Q. Kang, "Magnetic Quantum Cellular Automata-Based Logic Computation Structure: A Full-Adder Study," *Journal of Computational and Theoretical Nanoscience*, vol. 9, pp. 621-625, 2012.
- [14] D. B. Carlton, N. C. Emley, E. Tuchfeld, and J. Bokor, "Simulation Studies of Nanomagnet-Based Logic Architecture," *Nano Letters*, vol. 8, pp. 4173-4178, Dec 2008.
- [15] Hesjedal, T.; Phung, T., Magnetic logic element based on an S-shaped Permalloy structure. *Applied Physics Letters* 2010, 96 (7), 072501.
- [16] M. T. Niemier, E. Varga, G. H. Bernstein, W. Porod, M. T. Alam, A. Dingler, et al., "Shape Engineering for Controlled Switching With Nanomagnet Logic," *IEEE Transactions on Nanotechnology*, vol. 11, pp. 220-230, 2012.
- [17] D. Carlton, B. Lambson, A. Scholl, A. Young, P. Ashby, S. Dhuey, et al., "Investigation of Defects and Errors in Nanomagnetic Logic Circuits," *IEEE Transactions on Nanotechnology*, vol. 11, pp. 760-762, 2012.
- [18] H. Dey, G. Csaba, X. S. Hu, M. Niemier, G. H. Bernstein, and W. Porod, "Switching Behavior of Sharply Pointed Nanomagnets for Logic Applications," *IEEE Transactions on Magnetism*, vol. 49, pp. 3549-3552, 2013.
- [19] E. Varga, M. T. Niemier, G. Csaba, G. H. Bernstein, and W. Porod, "Experimental Realization of a Nanomagnet Full Adder Using Slanted-Edge Magnets," *IEEE Transactions on Magnetism*, vol. 49, pp. 4452-4455, 2013.
- [20] C. Augustine, B. Behin-Aein, F. Xuanyao, and K. Roy, "A design methodology and device/circuit/architecture compatible simulation framework for low-power Magnetic Quantum Cellular Automata systems," in 2009 Asia and South Pacific Design Automation Conference, 2009, pp. 847-852.
- [21] Z. Li, B. S. Kwon, and K. M. Krishnan, "Misalignment-free signal propagation in nanomagnet arrays and logic gates with 45-clocking field," *Journal of Applied Physics*, vol. 115, p. 17E502, 2014.
- [22] Z. Gu, M. E. Nowakowski, D. B. Carlton, R. Storz, M. Y. Im, J. Hong, et al., "Sub-nanosecond signal propagation in anisotropy-engineered nanomagnetic logic chains," *Nat Commun*, vol. 6, p. 6466, Mar 16 2015.
- [23] Z. Li and K. M. Krishnan, "A 3-input all magnetic full adder with misalignment-free clocking mechanism," *Journal of Applied Physics*, vol. 121, p. 023908, 2017.
- [24] H. Cho and E. E. Swartzlander, "Adder Designs and Analyses for Quantum-Dot Cellular Automata," *IEEE Transactions On Nanotechnology*, vol. 6, pp. 374-383, 2007.
- [25] M. J. Donahue and D. G. Porter, "OOMMF User's Guide, Version 1.0," Interagency Report NISTIR 6376 (1999).
- [26] S. B.-v. Gamm, A. Papp, E. Egel, C. Meier, C. Yilmaz, L. Hei, et al., "Design of On-Chip Readout Circuitry for Spin-Wave Devices," *IEEE Magnetics Letters*, vol. 8, pp. 1-4, 2017.
- [27] J. C. Gartside, D. M. Arroyo, D. M. Burn, V. L. Bemmer, A. Moskalenko, L. F. Cohen, et al., "Realization of ground state in artificial kagome spin ice via topological defect-driven magnetic writing," *Nature Nanotechnology*, vol. 13, pp. 53-58, 2018/01/01 2018.
- [28] Z. Bin, Y. Xiaokuo, L. Jiahao, L. Weiwei, and X. Jie, "Reliability analysis of magnetic logic interconnect wire subjected to magnet edge imperfections," *Journal of Semiconductors*, vol. 39, p. 024004, 2018.
- [29] H. D. Arnold and G. W. Elmen, "Permalloy, a new magnetic material of very high permeability," *The Bell System Technical Journal*, vol. 2, pp. 101-111, 1923.
- [30] D. C. M. Rodrigues, A. B. Klautau, A. Edstrm, J. Ruzs, L. Nordstrm, M. Pereiro, et al., "Magnetic anisotropy in permalloy: Hidden quantum mechanical features," *Physical Review B*, vol. 97, p. 224402, 06/04/ 2018.
- [31] Alexandra Imre, Experimental Study of Nanomagnets for Magnetic Quantum-Dot Cellular Automata (MQCA) Logic Applications Doctoral Dissertation, 2005, University of Notre Dame
- [32] L. F. Yin, D. H. Wei, N. Lei, L. H. Zhou, C. S. Tian, G. S. Dong, et al., "Magnetocrystalline Anisotropy in Permalloy Revisited," *Physical Review Letters*, vol. 97, p. 067203, 08/09/ 2006.
- [33] S. Kaya, "Uniaxial Anisotropy of a Permalloy Crystal," *Reviews of Modern Physics*, vol. 25, pp. 49-53, 01/01/ 1953.
- [34] WieWib Software, "CleWin - a hierarchical layout editor," ed: MESA+ Research Institute at the University of Twente and Deltamask.
- [35] Gavagnin, M.; Wanzelboeck, H. D.; Beli, D.; Bertagnolli, E., Synthesis of Individually Tuned Nanomagnets for Nanomagnet Logic by Direct Write Focused Electron Beam Induced Deposition. *ACS Nano* 2013, 7 (1), 777-784.
- [36] M. Marco, G. Gianluca, T. Silvia, and C. Giovanni, "Magnetization dynamics of single-domain nanodots and minimum energy dissipation during either irreversible or reversible switching," *Journal of Physics D: Applied Physics*, vol. 50, p. 453002, 2017.
- [37] L. G. C. Melo, T. R. B. S. Soares, and O. P. V. Neto, "Analysis of the Magnetostatic Energy of Chains of Single-Domain Nanomagnets for Logic Gates," *IEEE Transactions on Magnetism*, vol. 53, pp. 1-10, 2017.
- [38] M. Colci and M. Johnson, "Dipolar Coupling Between Nanopillar Spin Valves and Magnetic Quantum Cellular Automata Arrays," *IEEE Transactions on Nanotechnology*, vol. 12, pp. 824-830, 2013.
- [39] Santhosh, S.; Sanghamitra, D.; Swati Ghosh, A.; Amit, A., Tunable intrinsic magnetic phase transition in pristine single-layer graphene nanoribbons. *Nanotechnology* 2018, 29 (45), 455701.
- [40] W. Wernsdorfer, "Quantum dynamics in molecular nanomagnets," *Comptes Rendus Chimie*, vol. 11, pp. 1086-1109, 2008/10/01/ 2008.